Measurement 148 (2019) 106933

Contents lists available at ScienceDirect

Measurement

journal homepage: www.elsevier.com/locate/measurement

A low-cost wireless system of inertial sensors to postural analysis during human movement

Talysson M.O. Santos [a,e,*], Márcio F.S. Barroso [e,*], Rodrigo A. Ricco [d], Erivelton G. Nepomuceno [e], Érika L.F.C. Alvarenga [b], Álvaro C.O. Penoni [c], Ana F. Santos [f]

[a] Laboratory of Signal Processing (LPS-USP), Brazil
[b] Department of Natural Sciences (DCNAT-UFSJ), Brazil
[c] Department of the Sciences of Physical Education and Health (DCEFS-UFSJ), Brazil
[d] Department of Electrical Engineering (DEELT-UFOP), Brazil
[e] Control and Modelling Group (GCOM-UFSJ), Brazil
[f] Laboratory of Evaluation and Intervention in Orthopaedics and Traumatology (LAIOT-UFSCar), Brazil

ARTICLE INFO

Article history:
Received 2 January 2019
Received in revised form 6 June 2019
Accepted 12 July 2019
Available online 12 August 2019

Keywords:
Bio-mechanics
Human movements
Kinematics
Gait analysis
Inertial sensors
Complementary filter
Kalman filter
Wireless sensor network

ABSTRACT

The dynamics of the human body has generated considerable recent research interest among scientist devoted to reducing the number of injuries and for performance improvement. In these studies, the investigation is usually addressed by means of commercial devices based on video recordings. However, these systems based on video recordings are usually expensive and require suitable laboratories for their use, which makes it unfeasible to collect data for activities outside controlled environments. In this work, we have shown that it is possible to present similar results with a much lower sampling rate, focusing on the evaluation of minimum and maximum values of the gait. As a result, it has been possible to develop a wearable, compact, portable, low-cost, wireless and embedded system to simultaneously analyze the three-dimensional angular position in eight points. This technology can be used in many sorts of environments. It is also possible to access information in real time with reliable and accurate measurements by means of simple modelling for the use of fusion techniques implemented in the microcontroller. Tests were conducted to evaluate the metrological characteristics of the system using the Complementary Filter (CF) and the Kalman Filter (KF). An algorithm of evolutionary strategies tuned both filters, providing errors of less than 5% for static situations in the measurement of the angular position over the entire system utilization range. Our results have been compared with the commercial system Qualisys Motion-Capture. The statistical method elaborated by Bland and Altman has been used. We have found our method yields a motion analyses in good agreement with results using post-processed video.

1. Introduction

During the last few decades, running has gained popularity in recreational and competitive forms [1]. In 2017, about 65 million Americans practised this sport.[1] In recreational and competitive forms, there is a large percentage of musculoskeletal injuries associated with walking and running. Considering that the altered movement of joints cause these lesions [2], the biomechanical analysis of human movement has been used in several works [3–5] to reduce the number of injuries [6–8] and for performance improvement [9–11]. The most used method in the study of human movement is the analysis based on video recordings [12]. This method consists of multiple cameras to track the movements of the highlighted limbs with markers. These images are processed and analyzed using specific software, e.g. Visual 3D, to extract the kinematic data [13,14]. However, these systems are expensive and require suitable laboratories for their use, which makes it unfeasible to collect data for activities outside controlled environments [15].

To overcome these limitations presented based on video recordings, several methods and algorithms have been developed to analyze the dynamics of human movement by means of inertial sensors. Recently, an extensive review has been carried by [16]. In this work, more than 5000 works have been investigated, while 47 have been detailed analyzed. From this work, the following

* Corresponding authors at: Laboratory of Signal Processing (LPS-USP), Brazil (T.M.O. Santos).
E-mail addresses: talyssonsantos@usp.br (T.M.O. Santos), barroso@ufsj.edu.br (M.F.S. Barroso).
[1] https://www.statista.com/statistics/227423/number-of-joggers-and-runners-usa/.

https://doi.org/10.1016/j.measurement.2019.106933
0263-2241/

papers can be pointed out to evidence some investigations on methods and algorithms. In [17], a mathematical model named joint angles generation using optimization (JAGO) was proposed for human joint angle time-history generation. The JAGO model is based on an optimisation algorithm. Their structure is elaborated upon, and optimal values of the algorithm parameters are derived to achieve its robustness and result accuracy. A benchmark motion was used in a simulation exercise. As results, the maximal root mean square difference over time between estimated and benchmark quantities were around 1% of the peak to peak value for ground reaction components and intersegmental couples and 6% for a joint angles. In [18], the authors proposed an optimization algorithm for joint mechanic estimate using inertial measurement unit (IMU) data during a squat task, focusing on the ankle, knee and hip joints. The method is based on an optimal motor control strategy. Experiments were performed using 10 volunteers. Results show that normalized root mean square difference (%) is 3.5 ± 2.2 for ankle angle, 9.3 ± 4.5 for knee angle and 9.4 ± 4.8 for hip angle. Also in [19], an orientation algorithm was used to support a wearable inertial human motion tracking system for rehabilitation applications. The algorithm uses a quaternion representation. This representation, allowing accelerometer and magnetometer data to be used in an analytically derived and optimised gradient descent algorithm to compute the direction of the gyroscope measurement error as a quaternion derivative.

Due to the possibility of using algorithms to improve the performance of the inertial sensors, microelectromechanical magneto-inertial sensors (MEMs) which are inexpensive non-invasive sensors with small dimensions [20] have been widely used to analyze human movement in several works [21]. The authors in [22] have developed a wireless real-time human motion analysis device. They use the Digital Motion Processor (DMP) to extract the 3-D orientation data using quaternions to combine the accelerometers and gyroscopes data. The system consists of two inertial units connected to the controller via cable, and the controller wirelessly sends the information to the computer. The authors suggest using the Complementary Filter (CF) or Kalman Filter (KF) to obtain reliable and accurate orientation data to calculate the positions. The authors in [23] proposed a method to estimate gait parameters using inertial sensors. The parameters were estimated using the KF to fuse the data of accelerometer with the data of gyroscope. Besides, according to the authors, the most positive aspect of the work is the possibility of analyzing up to 5 points simultaneously. The system's inertial sensors are connected via cable to the controller, and the information is stored on a memory card. The authors pointed out that they had problems aligning the sensors and this caused measurement errors and the system does not allow the analysis of the information in real time. [24] make the use of inertial sensors for the classification of rehabilitation exercises. A wireless 9DoF IMU sensor was secured to the leg that was being exercised for data collection. Seven different lower limb rehabilitation exercises for a knee or hip injury was used. During the data acquisition, a sampling rate of 100 Hz was used. The available signal was filtered using 4th order low-pass Butterworth filter with a cut-off frequency of 20 Hz. As results, the authors obtained an accuracy score between 0.93 and 0.95 using principal component analysis (PCA).

Nowadays there are a considerable number of commercial inertial measurement unit (IMU) based systems to 3D motion tracking (e.g. Xsens company and Inertia Technology company). Xsens is the leading innovator in 3D motion tracking technology and products. Their systems were used in different applications like to model-based inverse dynamics using exclusively inertial motion capture (IMC) input, applicable in ambulatory environments and validate it against a conventional laboratory-based approach with 17 sensors node [25], to analyze kinematics and shock attenuation during a prolonged run on the athletic track with 8 sensors node [26] and to visual semantic landmark-based robust mapping and localization for autonomous indoor parking [27]. Inertia Technology is specialized in the development of miniaturized wireless devices that can sense, process and communicate motion, vibration and orientation features of interest. Their systems were used to examination of horse gait with 4 sensors nodes [28] and to stride detection in Warmblood horses at walk and trot with 8 sensors nodes [29].

The aforementioned commercial devices have been extensively used to investigate causes of injuries, such as the patellofemoral pain (PFP), which is one of the most common overuse running injury in the knee joint. One of the methods to investigate the causes of PFP has been to observe the rearfoot strike pattern by analyzing human movement based on video recordings. This strategy has been applied usually using commercial devices with sampling rate with around 200 Hz [30,31,14]. However, the information for gait patterns corresponds to 0.6–5.0 Hz [32–35]. Moreover, in a recent study, the maximal sprint velocity kinematics of the fastest 100 m sprinter Usain Bolt was investigated [36]. For data extraction, the computer program APAS (Ariel Performance Analysis System, Ariel Dynamics Inc., Coto de Caza Trabuco Canyon, USA) was used to reconstruct a 2D full-body biomechanical model. The coordinate data were smoothed using a low-pass filter with 14 Hz cut-off frequency. As results, Bolt presented a stride frequency of 4.16 Hz and his competitors also presented a stride frequency less than 5 Hz.

Taking into account the low frequency that the human movement presents during the gait, we have shown that it is possible to present similar results to analyzing human movement with a much lower sampling rate than the rate utilized in the analysis based on video recordings. Our focus is on the evaluation of minimum and maximum values of the gait using a sample rate of 20 Hz at each point of analysis. As a result, it has been possible to develop a wearable, compact, portable, low-cost and embedded system has been proposed to analyze the posture during human movement. The posture is analyzed from the measurement of the three-dimensional angular position at eight points simultaneously that communicate wirelessly to a receiver coupled to a nearby computer. Each of the eight nodes (inertial unit), is composed of an inertial sensor (made of accelerometers, gyroscopes, magnetometers), a microcontroller and a radio transceiver. CF and KF have been used to fuse the data from the sensors and get reliable measurements of the three-dimensional angular position. This approach presents three main features: the ability to be used in any environment, the ability to access information in real time and a simple modelling for the use of fusion techniques implemented in the microcontroller for reliable and accurate measurements. Additionally, the system has a graphical interface that facilitates analyzing the data in real time and allows to save the collected data.

Performed tests show that the use of CF and KF reduced the high error in the measurement of the angular position presented in works which use Quaternions [22,37]. The first step was to choose the best performance between the CF and KF fusion methods. After that, we have compared the proposed system to a well-established Qualisys Motion-Capture commercial system for the usual running on the treadmill. To describe agreement between the measurements of the two systems, Bland and Altman (BA) methodology [38] has bee used. BA method describes the agreement between two quantitative measurements by constructing limits of agreement. This statistical method has been used to validate spatiotemporal gait analysis using dual laser range sensors [39], the commercial system Equimoves (Inertia Technology company) for objective examination of horse gait [28] and in validation of inertial measurement units for upper Body Kinematics [40].

The remainder of this paper is organized as follows. Section 2 presents the fundamental concepts necessary for the use of the inertial sensors in the measurement of the angular position and the concepts of the techniques of sensor fusion. Section 3 presents the methodologies used in the fusion of the inertial sensors, the method used to optimize the sensor fusion, the characteristics of the proposed wireless network, the description of the tests performed to verify the metrological characteristics of the system and the standard test to apply the system in the analysis of human gait. Section 4 presents the results obtained for the tests described in Section 3. Finally, Section 5 presents the discussions and conclusions of this paper.

2. Background

2.1. Coordinate system

The coordinate system adopted is the NED industrial standard [41]. In this coordinate system, ϕ is the angle around the axis x called roll angle and its positive direction points to the north (N). θ is the angle around the y axis called pitch angle and its positive direction points to the east (E). ψ is the angle around the z axis called yaw angle and its positive direction points to down (D).

2.2. Inertial sensors to measure angular position

The gyroscope is a sensor which measures angular velocity (ω). The angular position in each of the three axes is the integrating the values of the angular velocity concerning time

$$\begin{bmatrix}\phi_{gi}\\ \theta_{gi}\\ \psi_{gi}\end{bmatrix} = \begin{bmatrix}1 & 0 & 0\\ 0 & 1 & 0\\ 0 & 0 & 1\end{bmatrix}\begin{bmatrix}\phi_{gi-1}\\ \theta_{gi-1}\\ \psi_{gi-1}\end{bmatrix} + \begin{bmatrix}T & 0 & 0\\ 0 & T & 0\\ 0 & 0 & T\end{bmatrix}\begin{bmatrix}\omega_{\phi i}\\ \omega_{\theta i}\\ \omega_{\psi i}\end{bmatrix},$$

where T is the sampling period.

The accelerometer measures linear acceleration and the acceleration of gravity. The acceleration projections on the accelerometer axes (a_x, a_y and a_z) can be used to measure angular position. The angle ψ cannot be measured because for motions around the z axis the acceleration of gravity does not change. The angles ψ and θ are calculated as

$$\begin{aligned}\phi_a &= \text{sen}^{-1}(a_y),\\ \theta_a &= \text{tg}^{-1}\left(\frac{a_x}{\sqrt{a_y^2+a_z^2}}\right).\end{aligned}$$

The magnetometer is a sensor that measures the direction and magnitude of the magnetic field. In applications involving human motion measurement, this sensor can be used to determine the angle ψ with the projections of the magnetic field on the axes (X_m, Y_m and Z_m). The magnetometer correctly estimate the angular position when the slope variation is compensated. In this work, this compensation was made with the angular position data of the accelerometer

$$\psi_m = \text{tg}^{-1}\left(\frac{Z_m\text{sen}\phi_a - Y_m\cos\phi_a}{X_m\cos\theta_a + Y_m\text{sen}\theta_a\text{sen}\phi_a + Z_m\text{sen}\theta_a\cos\phi_a}\right).$$

For the use of the equations previously presented, it is very important to calibrate the magnetometer [42]. This sensor must present the same gains for the three axes, so that by performing arbitrary rotations around the sensor axes, the collected values must form a sphere whose centre has null values. The process of calibration and elimination of distortions affecting magnetometer measurements is described in [43].

2.3. Sensor fusion

Sensors fusion is used to estimate the state of a system from data collected using two or more sensors. As MEMs inertial sensors have particular limitations and errors when working separately to measure angular position, in this work the CF and the KF have been used to combine the information of the gyroscope with accelerometer to estimate the angles ϕ and θ, and for combining the information from the gyroscope with the magnetometer to measure the angle ψ.

The CF aims to explore characteristics of the frequency response of the sensors considering the most reliable frequency spectra of each sensor to combine information that is at different and complementary frequencies without distorting the signal. The schematic diagram in Fig. 1 illustrates the CF in the discrete domain.

KF is a set of mathematical equations that form a filtering algorithm that estimates states and is called a predictor-corrector. Although the KF is defined for continuous systems, in this work, only the discrete case has been used. The function of the KF is trying to estimate the state $x \in \mathbb{R}^n$ of a controlled process in discrete instants of time and which can be represented by the process Equation (x_i) and measurement Equation (y_i)

$$\begin{aligned}x_i &= Ax_{i-1} + B\omega_i + z_i,\\ y_i &= Hx_{ri} + v_i,\end{aligned}$$

where $x_i \in \mathbb{R}^n$ is the vector of angular positions estimated by KF, $x_{ri} \in \mathbb{R}^n$ is the vector of angular positions from the accelerometer and magnetometer, $\omega_i \in \mathbb{R}^p$ is the vector of angular velocities in the three axes obtained by means of the gyroscope, $A \in \mathbb{R}^{n\times n}$ is the state transition matrix, $B \in \mathbb{R}^{n\times p}$ is the matrix that models the associated input, $y_i \in \mathbb{R}^{m\times 1}$ is the vector of measures, $H \in \mathbb{R}^{m\times n}$ is the matrix that models the states associated with measurement that are derived from the accelerometer and magnetometer data, $z_i \in \mathbb{R}^{n\times 1}$ is the process noise e $v_i \in \mathbb{R}^{m\times 1}$ is the measurement noise.

The matrices A, B and H determine how the KF was modelled for the process and the type of adopted model. If they are diagonal matrices, it means that the variables to which they are associated are considered independent and are not directly related. In this work, the model adopted is linear, and the matrices are diagonal. A and B are identity matrices, and H has the sampling period on the main diagonal. Therefore, the discrete linear model of KF was used. KF consists of two main steps: the first of prediction and the second of correction, as can be seen in the diagram of equations of the linear KF illustrated in Fig. 2.

2.4. Evolutionary strategies – ES

The performance of the sensor fusion algorithms depends on the correct choice of their parameters. An algorithm of Evolutionary Strategies is applied to optimize the choice of these parameters

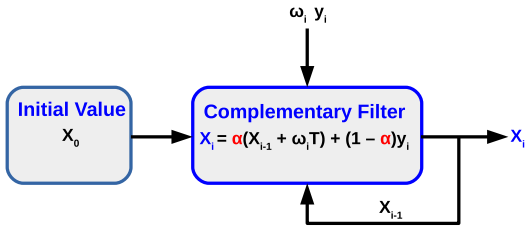

Fig. 1. Complementary filter used to estimate angular position. ω_i is the matrix containing the angular velocities measured by the gyroscope, T is the sampling period, y_i is the matrix with the angular positions estimated by the accelerometer and magnetometer and α is the only one performance parameter of the CF. α must be between 0 and 1. The closer to 1 the greater the reliability assigned to the gyroscope. α must be estimated for each of the three angular positions, and it is a diagonal matrix.

and consequently to improve the performance of the filters. ES is a class of evolutionary algorithms used mainly to solve problems of parameter estimation. An essential feature of ES is the self-adaptation of the parameters during the evolutionary process, by introducing them into the genetic representation of individuals [44]. Generation of new individuals is given by

$$x^{k+p} = x^k + \beta N x^k, \quad (1)$$

where p is the initial number of individuals of a population, k ranges from 1 up to p, x^k are the p initial individuals, x^{k+p} are the p individuals being generated, β is the mutation rate, N is a probability density function used for the process of self-adaptation of individuals.

3. Materials and methods

3.1. Optimization of CF and KF

As emphasized in the previous section, the performance of the CF depends only on α and the performance of the KF depends on R and Q. R was determined by the error of the angular positions of ϕ, θ and ψ from the accelerometer and magnetometer. For this, 20 acquisitions of 2 min with a sampling rate of 20 Hz were performed with the instruments stopped in 0°, and the mean of the results was obtained.

Given the R values for each of the axes, the optimal KF tuning becomes dependent only on Q, just as the optimal tuning of the CF depends only on α. These parameters are estimated from the proposed algorithm of Evolutionary Strategies represented by the pseudo-code in Algorithm 1.

Algorithm 1 Optimization of CF and KF by ES.

```
data ← angular velocity (gyroscope) and angular position (accelerometer or magnetometer)
auxiliary ← 0
best_previous ← 0
min_error ← 1000000
parameter ← population of 5 random individuals
while auxiliary < 20 do
  for i = 1:length(parameter) do
    parameter (i + 5) ← parameter(i) + 0.01*N*parameter (i)
  end for
  for j = 1:length(parameter) do
    for i = 1:length(data) do
      angular_position ← angular position estimated by the filter
    end for
    quadratic_error ←sum(angular_position − 0)^2
    if quadratic_error < min_error then
      best_parameter ← parameter (j)
      min_error ← quadratic_error
    end if
  end for
  if best_previous==best_parameter then
    auxiliary ← auxiliary +1
  end if
  parameter ← population of 5 individuals: the best of past generation, 3 drawn of 10 and 1 random
end while
```

Before using the proposed algorithm to determine the performance parameters of the filters, the stability has been tested by means of the data set from the angular position of the accelerometer and the angular velocity of the gyroscope. The algorithm has been tested 20 times with the same data set. If in all twenty times the algorithm converged to near points of optimal tuning, i.e., it presented low standard deviation, it means that the algorithm is stable. Otherwise, the algorithm is not stable and is returning random solutions or local optimal solutions.

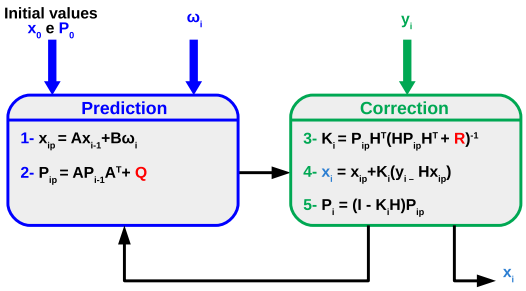

Fig. 2. Kalman filter used to estimate angular position. x_{ip} is the priori process state, P_{ip} is the priori error covariance, Q is the covariance of the process noise, R is the covariance of the measurement noise, K is the Kalman gain, x_i is the corrected state (angular positions) and P_i is covariance of the error. The Kalman gain reduces the covariance of the error and depends on R and Q which are the performance parameters of the KF.

In addition, to compare if the developed algorithm is actually converging to optimal solutions, a exhaustive search algorithm has been implemented that tests all values of α that are in the range of 0.1 to 1, with step of 0.0001 and all values of Q which are in the range of $\frac{R}{1000}$ to 1, with step of 0.00001. In this way, it is possible to compare the results obtained to analyze the computational cost of the two algorithms and the efficiency of the proposed tuning method. The criterion to determine the optimal value of α and Q is the same for the two algorithms, which is the value of α and Q that result in the least sum of the quadratic error for a data set.

These algorithms were implemented using a Jupyter Notebook interface for Python3. The parameters of the filters were determined using a set of 20 data collections with the static instrument at 0°. This data set consists of the three-dimensional angular velocity reported by the gyroscope and the angular position reported by the accelerometer (for ϕ and θ) and magnetometer (for ψ). The codes were run on a notebook with Intel (R) Core i3 M350 2.27 GHz processor, 4 Gb RAM and Linux Lite 4.0 operating system.

3.2. Tests for metrological analysis of the system

After finding the performance parameters of CF and KF, tests were applied to analyze the metrological characteristics of the system and to verify which of the two filters had the best performance.

3.2.1. Measurement in 0°

The objective of the test with the instrument stopped at 0° is to compare the static behaviour of the sensors isolated use of the sensors with the use of sensors combined by CF and KF. In this test, it is possible to verify the mean value (accuracy) and the standard deviation of the measurements (precision). For this purpose, the angular position estimated by the accelerometer, gyroscope and magnetometer working in isolation and the angular position obtained with the use of CF and KF were collected 20 times during 2 min with a sampling rate of 20 Hz.

3.2.2. Dynamic characteristics of instruments

The objective of the test is to analyze the dynamic behaviour of the sensors isolated and combined by CF and KF during fast varia-

tions of angular positions. To vary the angular positions, a rod was coupled to a servo motor and the inertial unit was fixed on the rod for the tests. The schematic of the test platform can be seen in Fig. 3. The servo motor has speed rate of 0.22 s/60°.

3.2.3. Error curve

Ideally, the indication presented by a measurement system should correspond to the actual value of the measurand. However, no matter how good the quality of the measurement system, the measurement error exists. In this sense, the measurement error cannot be ignored in reliable measurement processes, and it is necessary to estimate the error curve to graphically represent the error distribution over the entire range of use of the angular measurement instrument on the three axes.

The error curve represents the systematic and random errors of a measurement system and can be estimated from the trend and repeatability of the instrument. The trend represents systematic errors and it is obtained from the difference in the mean of a finite set of instrument indications relative to the conventional true value of the measurand. The repeatability is the range of values symmetric, around the mean value, within which the random error is expected with some probability and is calculated by the product of the standard deviation by the respective Student's t coefficient. To determine the error curve in this work, the *t* test was applied using a probability of 95.45% and 15 degrees of freedom (16 points collected). With these values of probability and degrees of freedom, we have the corresponding Student t coefficient equal to 2.181.

To vary the angular positions and estimate the errors throughout the range of use of the instrument, the test platform illustrated in Fig. 3 was used. The choice of the servo motor is related to its operation. As it has a feedback system powered by a potentiometer that acts as a shaft position sensor, it can be used in applications where there is a need to move in a precise and controlled manner.

3.3. Wireless sensor network

The complete system consists of a wireless network of 8 inertial units. Each inertial unit consists of 1 MPU9250 (inertial sensors: accelerometer, gyroscope and magnetometer), 1 ATMEGA328 microcontroller and 1 NRF24L01 (radio transceiver), as shown in the Fig. 4.

The proposed network is a master-slave network and is shown in Fig. 5. The master is the receiver and is responsible for coordinating the sending of all 8 sensors that form the network. For this, each emitter is identified by a tag and has its own address. The receiver points to which node will send the information, checks if the connection has been established and checks to see if it has received the information and the tag of the emitter. If there is a problem, such as a lack of connection, the receiver stops at the faulty node and it is easily to identify which unit is faulty. The receiver is coupled to the computer and consists of an ARM Cortex-M3 microcontroller and an NRF24L01 module.

The receiver coordinates the amount of information that is sent by each inertial unit. This organization of the amount of information sent at a time occurs in function of the time that is spent to make the acquisition of all elements of the network and the time of sampling of each inertial unit.

Before sending, each inertial unit converts the angular positions to integer values. This conversion is to send more information in each time. The communication module allows sending 32 bytes at a time and, in the Arduino platform, each float type number occupies 4 bytes and the integer type 2 bytes. For example, if the time spent to traverse all emitters is 0.25 s and the sampling rate of each inertial unit is 20 Hz, every 0.25 s each inertial unit sends 5 angular position data of the x, y, and z-axes. In addition, each

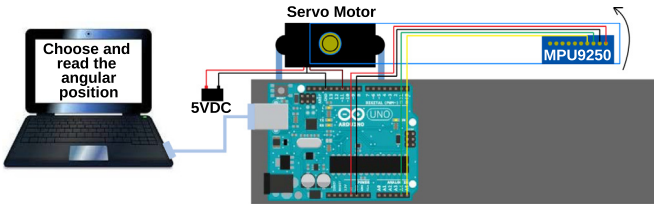

Fig. 3. Platform for tests. The platform is composed of a rod coupled to the servomotor, that allows to vary the angular position in a fast and controlled way.

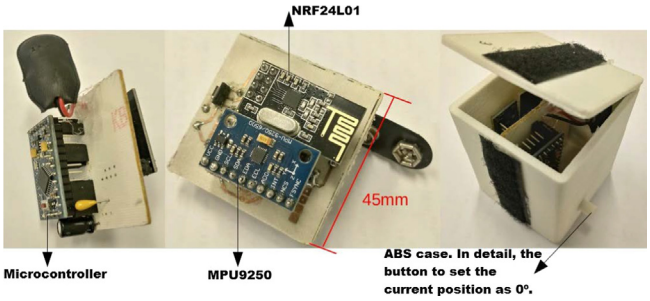

Fig. 4. Inertial unit. In this image, the following components are described. The microcontroller responsible for processing the data, the inertial sensor that consists of accelerometer, gyroscope and magnetometer, the module for transmitting wireless information NRF24L01 and the system shipped in the ABS box with the button to choose the position in which it is as zero degree. The system is powered by a 9-volt battery.

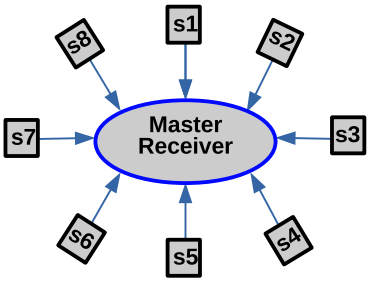

Fig. 5. Network of the slave master type composed of 8 inertial units represented by s1-s8. All elements of the network are controlled by the receiver and form a versatile, low cost system that allows three-dimensional angular analysis in 8 points simultaneously.

emitter has an identification tag to send angular position information. At the same time, 1 integer is transmitted to identify the network device, 5 integers of angular position of the x-axis, 5 of the y-axis and 5 of the z-axis, totalling 32 bytes in each package.

3.4. Application of the system: gait analysis

The complete system was used during the usual running on the treadmill *MovementLX*160. The test was performed at speed of 4.5 km/h during 90 s. The objective of the test is to analyze the kinematic data of the trunk, pelvis, hip, knee and ankle during the gait. One physically active subject (age: 23; height: 175 cm; weight: 70 kg) volunteered to participate in the study. Fig. 6 shows the inertial units positioned in the voluntary.

To compare the data of the proposed system, the same test was performed using the Qualisys Motion-Capture commercial system. For this, the kinematic data collection used 7 motion analysis cameras (Qualisys Motion-Capture System, Qualisys Medical AB, Sweden). The software Qualisys Track Manager (Qualisys Medical, AB, Sweden) and Visual 3D (Version 3.9; C-Motion Inc., Rockville, USA) was used for reconstruction and quantification of kinematics

through the joint coordinate system. Data were filtered using a low-pass, fourth-order Butterworth filter with zero phase delay and the cut-off frequency of 12 Hz. Cardan angles were calculated using the coordinate system definitions recommended by International Society of Biomechanics [45] relative with static posture. Fig. 7 illustrates the 20 reflective markers located on anatomical landmarks and 5 cluster tracking markers which are placed on the participant to perform the test.

After applying the same test with the same individual in the two systems, a measurement comparison of the proposed system with the Qualisys Motion-Capture Commercial system was performed. For this, the statistical method of Bland–Altman for assessing agreement between the two methods of clinical measurement was applied [38].

4. Results and discussion

Fig. 8 shows the results of the test of stability of the proposed algorithm.

Fig. 8 shows that the ES algorithm is stable because it presents a low variation of the results obtained for the repeated analysis of the same data set. The average value found for α and Q by the ES algorithm is very close to the value found by the exhaustive search algorithm (EX). The ES algorithm found an average of α equal to 0.87397 and EX found α equal to 0.87780. For Q, ES found an average equal to 0.00031 and EX found Q equal to 0.00027. Therefore, the proposed algorithm is converging to global optimal solutions. The great advantage of the proposed algorithm is that its execution time is much smaller than exhaustive search algorithms. The average time to find the α parameter was approximately 1.7 seconds and 2.6 seconds for Q. For the same data set the ES algorithm spent approximately 46 s to estimate α and 1192 s for Q.

After verifying that the proposed ES algorithm presents satisfactory performance and finds the solutions quickly, the parameters of the CF and KF were determined according to the Section 3.1. The results are in Table 1.

The results presented in Table 1 shows that the greatest reliability is in the gyroscope because for the CF α is close to 1 and for the KF $Q \ll R$. The accelerometer and magnetometer have noisy measurements of angular position, consequently, as the optimization algorithm prioritizes the smallest sum of the quadratic error, the greatest reliability is of the gyroscope.

After determining the optimum CF and KF parameters, tests to check the system performance were applied. Table 2 contains the 95% confidence interval of the 20 set of data collected with the static system at 0°.

In Table 2, it is possible to observe that the two filters presented good results. Measures have become more precise and accurate using the filters than with the instruments working alone. The KF was superior in relation to the CF for the estimation of the three angles, leaving the readings with lower standard deviation and with the average closer to the expected value.

Using the KF there was a reduction of 27.24% in the trend of the instrument for measurement around the x-axis, 13.13% for the y-axis and 1.31% for the z-axis. In addition, the instrument became more precise, as the standard deviation reduced 74.19% for the roll angle, 73.45% for pitch angle and 87.36% for the yaw angle, showing the efficiency of the filter for sensor fusion. Analyzing the confidence interval, it is observed that the length of the interval is smaller for KF and CF, that is, they have less dispersion. However, although the accelerometer interval was larger, it also performed well.

Fig. 9 shows the measurement of the angular position with fast variation of position. The general behaviour associated with the data presented in Table 2, is illustrated on static parts of the figure.

Fig. 6. Proposed system positioned for angular analysis of the trunk, hip, knee and ankle during gait.

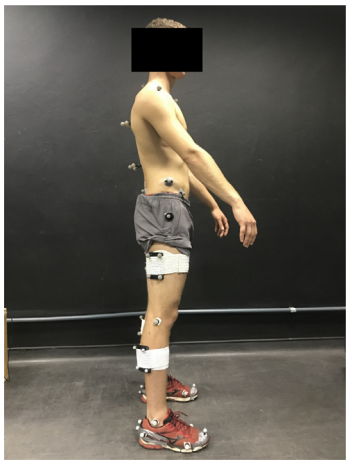

Fig. 7. Positioning the markers to use the Qualisys Motion-Capture Commercial system.

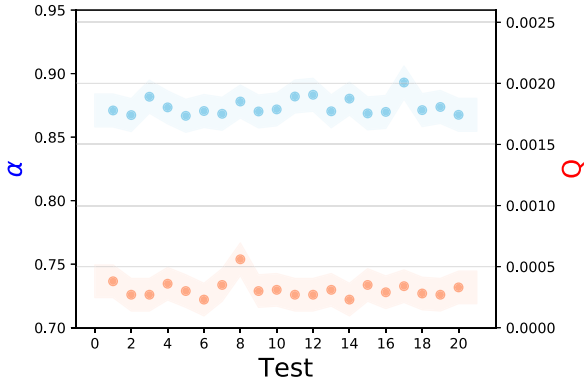

Fig. 8. Algorithm performance: results using the same dataset 20 times. Blue polka dots represent the values found to α for each of the 20 tests. Orange polka dots represent the values found to Q. The scale on the left at y-axis corresponds to values of α. The scale on the right corresponds to Q values.

Analyzing Fig. 9, the accelerometer presents overshoot at fast angular position change because its operating principle is based on a mass-spring type system. The gyroscope presents bad accuracy. The dynamic response of the system presents a good performance with CF and KF, eliminating the overshoot presents by the

Table 1
Optimum CF and KF parameters estimated using the average value of the 20 runs using a different set of data in each execution. Each set of data was collected during 2 min with rate of 20 Hz and with the instrument static in 0°.

Parameter	Roll	Pitch	Yaw
α	0.8103	0.8904	0.9533
R	0.0104	0.0155	0.0874
Q	0.000149	0.000196	0.00008

Table 2
Results (in degree) of the angular measurement in 0°. CI stands for the Confidence Interval.

Angle Measurement	Roll 95%CI	Pitch 95%CI	Yaw 95%CI
Acel. or Magn.	-0.08 ± 0.06	0.06 ± 0.06	-0.33 ± 0.64
Gyroscope	2.21 ± 0.55	-1.33 ± 0.33	-2.47 ± 0.66
CF	-0.06 ± 0.02	0.05 ± 0.02	-0.37 ± 0.1
KF	-0.06 ± 0.01	0.05 ± 0.02	-0.33 ± 0.08

accelerometer. The dynamic response is better with the use of KF because it presents a shorter response time than the CF.

Even using the sensor fusion algorithms and obtaining measurements with good precision and accuracy, all systems have measurement errors that must be predicted. Fig. 10 illustrate the expected error for the roll, pitch and yaw angles using CF and KF.

Analyzing the error curves, with 95.45% probability, the angular measurement error for the roll angle is expected to be between $-0.81°$ and $0.90°$ for the CF and between $-0.80°$ and $1.11°$ for KF. For the pitch angle, the expected error is between $-1.17°$ e $0.88°$ for CF and between $-0.91°$ and $0.90°$ for KF. The expected error for yaw angle is between $-1.32°$ and $1.59°$ for CF and -1.00 and $1.35°$ for KF.

After applying tests to verify the metrological characteristics of the system in static situations, it was observed that the KF presents better performance than the CF and was chosen to be used in each of the 8 units that compose the system. For the static tests applied, using the KF, an error of less than 5% in angular measurement is expected, which is a significant improvement over the results of the work of [22], where the expected error in the angular position measurement was 17–24%.

As a final test, the complete system was applied for postural analysis during gait and the result was compared to that obtained by the Qualisys capture system. Gait is a cyclical exercise and our objective was only to evaluate the maximum and minimum values. Determining the minimum and maximum values of cyclic exercises, within normalities, these values would be maintained throughout the training and would be sufficient to characterize the movement. The movements were analyzed in the 3 anatomical planes: frontal (x), sagittal (y) and transverse (z) planes. The angular positions of x, y and z planes are represented with the ϕ, θ and ψ angles respectively. The results are shown in Table 3.

It is possible to notice in Table 3 that right and left ankle pitch and yaw measurements present an inferior agreement with the Qualisys system when compared with other measurement. Since the inertial unit has been placed on the instep and we had difficulty to fasten it without causing discomfort, the instrument has been in movement and consequently, errors in pitch and yaw angle measurements occurred.

To demonstrate the spread of differences of the individual pairs in each parameter, Bland-Altman plots were used. Fig. 11 illustrates the limits of agreement between the proposed system and the Qualisys system. All limits were determined without 'linear' attempt to model and remove a multiplicative offset between each assay by linear regression and without 'ODR' attempt to model and

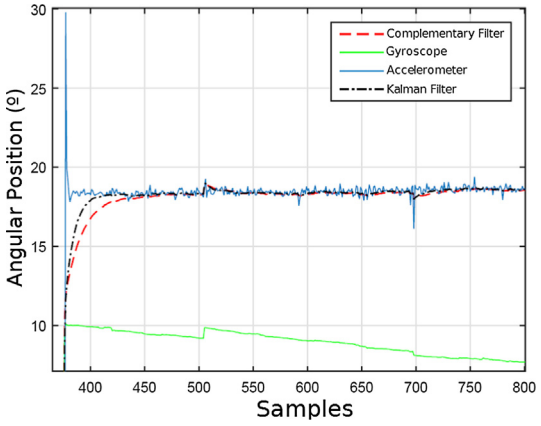

Fig. 9. Excerpt of the measurement of angular position with fast change of position. During the transition of the angular position, the accelerometer presents overshoot. During the static part, the gyroscope accumulates integration errors presenting drift and low accuracy. The behaviour of the magnetometer is similar to the accelerometer. The use of CF and KF makes measurements more precise and accurate, without noise or drift during the static intervals and without overshoot during the dynamic intervals. The response time of KF is lower than that of CF.

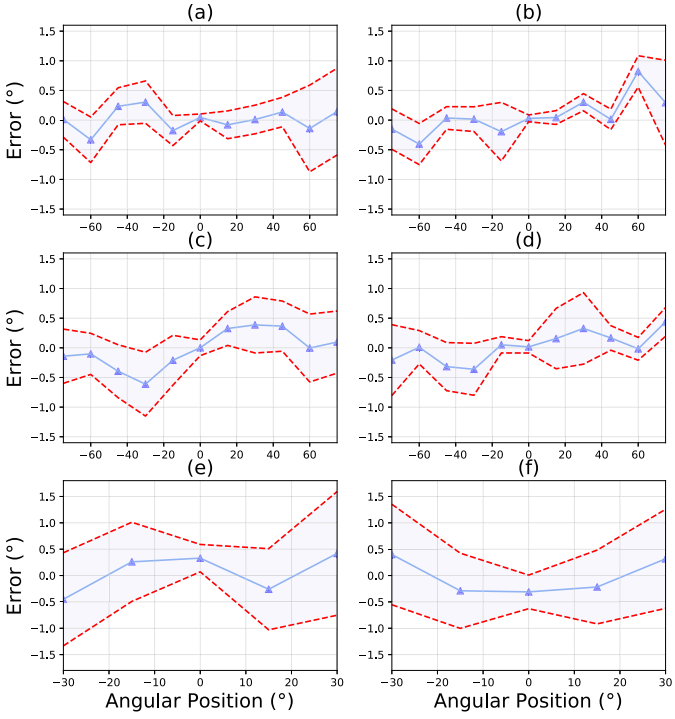

Fig. 10. Error curve. First line roll angle: a) CF and b) KF; Second line pitch angle: c) CF and d) KF; Third line yaw angle: e) CF and f) KF. The dashed line represents the trend of the error. The hatching region is the interval that the error will be with 95.45% probability. The upper limit of the hatched area is the sum of the trend with the repeatability and the lower limit is the subtraction of the trend with repeatability.

remove a multiplicative offset between each assay by orthogonal distance regression. Right and left ankle pitch and yaw measurements did not enter BA analysis because they presented the problems described previously.

The authors of [28] have employed a commercial inertial system (Inertia Technology company) to evaluate horse gait and [40] utilized a commercial inertial system (APDM Wearable Technologies company) to evaluate upper body kinematics. Both works

Table 3
Results of the angular measurement (in degree) during the gait at 4.5 km/h.

Segment	Developed System						Qualisys System					
	Roll (ϕ)		Pitch (θ)		Yaw (ψ)		Roll (ϕ)		Pitch (θ)		Yaw (ψ)	
	min	max	min	max	min	max	min	max	min	max	min	max
Trunk	−3	11	−6	7	−18	13	3	11	−2	5	−8	4
Pelvis	−1	7	−6	3	−23	5	0	6	−3	1	−8	5
Left Hip	−19	30	−13	7	−14	23	−25	28	−9	1	−22	14
Right Hip	−16	25	−10	10	−23	13	−21	27	−6	12	−18	8
Left Knee	−14	57	−14	22	−10	27	−20	62	−5	14	−9	28
Right Knee	−16	57	−19	9	−26	15	−16	60	−13	5	−29	−5
Left Ankle	−32	9	−14	29	−17	14	−30	8	−5	13	−6	12
Right Ankle	−22	7	−16	22	−28	26	−19	11	−10	8	−24	−12

The references to the positive values of movement in each plane are state as follows. Trunk: ϕ (flexion), θ (ipsilateral inclination) and ψ (ipsilateral rotation). Pelvis: ϕ (flexion), θ (ipsilateral inclination) and ψ (ipsilateral rotation). Hip: ϕ (flexion), θ (abduction) and ψ (medial rotation). Knee: ϕ (flexion), θ (abduction) and ψ (medial rotation). Ankle: ϕ (dorsiflexion), θ (inversion) and ψ (medial rotation).

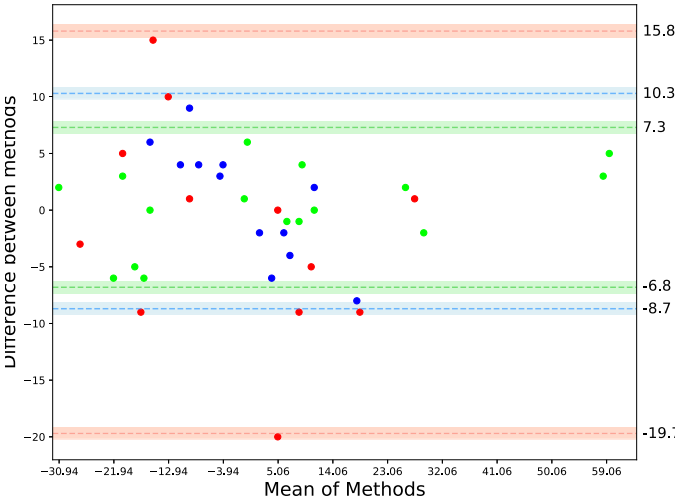

Fig. 11. Application of Bland and Altman method to evaluate the difference of two methods. Limits of agreement between the proposed system and the Qualisys system for measure angular position during the gait at 4.5 km/h. Markers with green polka dots represents the punctual differences between the measures of the systems for roll angle. Markers with blue polka dots represents the punctual differences for pitch angle. Red polka dots represents the punctual differences for yaw angles. Horizontal lines represent the limits of agreement between the methods. 95 % of the differences between the methods will be between the limits represented in the figure. The horizontal lines have the same colour pattern adopted for the markers.

used BA to compare with an optical motion capture system. Table 4 presents the results of Fig. 11 and the results presented by [28,40].

So, comparing with the other results obtained for the commercial inertial systems, which are more expensive than our system, the limits of the agreement obtained for roll and pitch angle shows that our system presents good results and consequently good agreement in relation with Qualisys system.

The results obtained for yaw angle presents worse results than the other two angles because the magnetometer have a worse performance than accelerometer for angular measurements. Another important feature of bio-medical instruments is the influence of the training factor on instrument measurement errors. During the first tests, the individual may not be accustomed to performing the activity with the instrument in their body. This can cause changes in exercise execution movements and increase the difference between the measurements of two systems.

5. Conclusions and recommendations

In this work, a low-cost wireless system to analyze the posture during human movement has been developed. The motivation to develop such device is due the fact that commercial solution are unaffordable for many researchers and professionals. For applications, such as those involved to observe the rearfoot strike pattern, we have shown the possibility to collect data in a lower sampling rate. It has been possible since the maximum and minimum values of the gait are sufficient to describe such pattern. The developed system can be used in several types of environments. It also allows access to information in real time. Moreover, as many tests have shown, its metrological characteristics are in a good agreement with commercial counterpart.

The system allows you to analyze angular position in eight points simultaneously in real time. Other systems described in the literature allow to analyze only 1 point in real time [22] and 4 points without real time analysis [23]. The tests to verify the quality of the measurements of the system were carried out successfully and presented good results. The expected error of angular position with 95.45% probability for static tests is close to 5% for both CF and KF use.

Finally, the complete system was used during a typical running on the treadmill *MovementLX*160. The test was performed at speed of 4.5 km/h. The objective of the test is to analyze the kinematic data of the trunk, pelvis, hip, knee and ankle during the gait to verify the performance of the system for dynamic analysis. A comparison with a commercial system Qualisys Motion-Capture is present in Table 3. The results are clearly correlated with the results using post-processed video. Additionally, we have compared our results

Table 4
Limits of agreement obtained by the Bland and Altman method: A comparison between our results with the presented in [28,40].

Angle	Developed System			[28]			[40]		
	Lower	Bias	Upper	Lower	Bias	Upper	Lower	Bias	Upper
ϕ	−6.8	0.2	7.3	−2.3	0.3	2.3	−6.2	0.8	7.9
θ	−8.7	0.8	10.3	−8.8	0.4	8.1	–	–	–
ψ	−19.7	−1.9	15.8	–	–	–	–	–	–

with other works in literature using the Bland and Altman method as can be seen in Table 4. For the angle ϕ, our method presents the lowest bias. The other values in Table 4 show that our method is at least comparable with other techniques in the literature.

Regarding the possible applications of the system, having the possibility to measure the range of movements using the maximum and minimum values is an excellent help in the treatment for injury rehabilitation. Usually, after the injury, the patient initiates the treatment with functional limitations, and it is important to follow the progress during the procedure with gradual restoration of movement. For example, anterior cruciate ligament (ACL) injuries often require intervention followed by an extensive course of rehabilitation because, without treatment, they frequently result in functional and athletic limitations [46]. In the context of high-level sport, the system can be used to improve the performance of athletes. [36] concluded that Usain Bolt compared to his competitors took fewer and less frequent strides, which was a deterministic factor in his 1st place finish. Therefore, it can be applied to try to adjust strides characteristics and consequently improve the performance.

Declaration of Competing Interest

The authors declare that they have no known competing financial interests or personal relationships that could have appeared to influence the work reported in this paper.

Acknowledgement

The authors wish to acknowledge the financial support given by FAPEMIG, CNPq and CAPES.

References

[1] R. Mann, L. Malisoux, A. Urhausen, K. Meijer, D. Theisen, Plantar pressure measurements and running-related injury: a systematic review of methods and possible associations, Gait Posture 47 (2016) 1–9.
[2] V.H. Chuter, X.A.K.J. De Jonge, Proximal and distal contributions to lower extremity injury: a review of the literature, Gait Posture 36 (1) (2012) 7–15.
[3] S. Qiu, Z. Wang, H. Zhao, K. Qin, Z. Li, H. Hu, Inertial/magnetic sensors based pedestrian dead reckoning by means of multi-sensor fusion, Inf. Fusion 39 (2018) 108–119.
[4] K. Cahill-Rowley, J. Rose, Temporal-spatial reach parameters derived from inertial sensors: comparison to 3D marker-based motion capture, J. Biomech. 52 (2017) 11–16.
[5] R. Ferber, S.T. Osis, J.L. Hicks, S.L. Delp, Gait biomechanics in the era of data science, J. Biomech. 49 (16) (2016) 3759–3761.
[6] K. Liu, J. Yan, Y. Liu, M. Ye, Noninvasive estimation of joint moments with inertial sensor system for analysis of STS rehabilitation training, J. Healthcare Eng. 2018 (2018) 1–15.
[7] A. Alizadegan, S. Behzadipour, Shoulder and elbow joint angle estimation for upper limb rehabilitation tasks using low-cost inertial and optical sensors, J. Mech. Med. Biol. 17 (2) (2017), 1750031 1-20.
[8] S.M. Sigward, M.-S.M. Chan, P.E. Lin, Characterizing knee loading asymmetry in individuals following anterior cruciate ligament reconstruction using inertial sensors, Gait Posture 49 (2016) 114–119.
[9] R.P. Olympia, H. Wakefield, B. Wakefield, C.J. Weber, Injuries depicted in sport-related films, Clin. Pediatr. 57 (9) (2018) 1033–1040.
[10] S. Ganzevles, R. Vullings, P.J. Beek, H. Daanen, M. Truijens, Using tri-axial accelerometry in daily elite swim training practice, Sensors 17 (5) (2017) 1–14.
[11] J.B. Shepherd, D.V. Thiel, H.G. Espinosa, Evaluating the use of inertial-magnetic sensors to assess fatigue in boxing during intensive training, IEEE Sens. Lett. 1 (2) (2017) 1–4.
[12] R. Mooney, G. Corley, A. Godfrey, C. Osborough, R. Newell, J. Quinlan, G. Olaighin, Analysis of swimming performance: perceptions and practices of us-based swimming coaches, J. Sports Sci. 34 (11) (2015) 997–1005.
[13] G.E. Kang, M.M. Gross, Concurrent validation of magnetic and inertial measurement units in estimating upper body posture during gait, Measurement 82 (2016) 240–245.
[14] A.F. Dos Santos, T.H. Nakagawa, G.Y. Nakashima, M.C.D.F. Serro, The effects of forefoot striking, increasing step rate, and forward trunk lean running on trunk and lower limb kinematics and comfort, Orthopedics Biomech. 37 (5) (2016) 369–373.
[15] G. Li, T. Liu, J. Yi, Wearable sensor system for detecting gait parameters of abnormal gaits: a feasibility study, IEEE Sens. J. 18 (10) (2018) 4234–4241.
[16] W. Johnston, M. O'Reilly, R. Argent, B. Caulfield, Reliability, validity and utility of inertial sensor systems for postural control assessment in sport science and medicine applications: a systematic review, Sports Med. 49 (5) (2019) 783–818, https://doi.org/10.1007/s40279-019-01095-9.
[17] C. Mazzà, A. Cappozzo, An optimization algorithm for human joint angle time-history generation using external force data, Ann. Biomed. Eng. 32 (5) (2004) 764–772, https://doi.org/10.1023/B:ABME.0000030241.26857.75.
[18] V. Bonnet, C. Mazz, P. Fraisse, A. Cappozzo, An optimization algorithm for joint mechanics estimate using inertial measurement unit data during a squat task, Annual International Conference of the IEEE Engineering in Medicine and Biology Society 2011 (2011) 3488–3491, https://doi.org/10.1109/IEMBS.2011.6090942.
[19] S.O.H. Madgwick, A.J.L. Harrison, R. Vaidyanathan, Estimation of IMU and MARG orientation using a gradient descent algorithm, IEEE International Conference on Rehabilitation Robotics 2011 (2011) 1–7, https://doi.org/10.1109/ICORR.2011.5975346.
[20] J.M. Lambrecht, R.F. Kirsch, Miniature low-power inertial sensors: promising technology for implantable motion capture systems, IEEE Trans. Neural Syst. Rehabil. Eng. 22 (6) (2014) 1138–1147.
[21] V. Camomilla, E. Bergamini, S. Fantozzi, G. Vannozzi, Trends supporting the in-field use of wearable inertial sensors for sport performance evaluation: a systematic review, Sensors 18 (3) (2018) 2–50.
[22] Z. Ong, Y. Seet, S. Khoo, S. Noroozi, Development of an economic wireless human motion analysis device for quantitative assessment of human body joint, Measurement 115 (2018) 306–315.
[23] K. Bötzel, A. Olivares, J.P. Cunha, J.M. Górriz Sáez, R. Weiss, A. Plate, Quantification of gait parameters with inertial sensors and inverse kinematics, J. Biomech. 72 (2018) 207–214.
[24] O. Giggins, K.T. Sweeney, B. Caulfield, The use of inertial sensors for the classification of rehabilitation exercises, in: 2014 36th Annual International Conference of the IEEE Engineering in Medicine and Biology Society, 2014, pp. 2965–2968.https://doi.org/10.1109/EMBC.2014.6944245..
[25] A. Karatsidis, M. Jung, M. Schepers, G. Bellusci, M. de Zee, P. Veltink, M. Andersen, Musculoskeletal model-based inverse dynamic analysis under ambulatory conditions using inertial motion capture, Med. Eng. Phys. 65 (2019) 68–77.
[26] J. Reenalda, E. Maartens, J.H. Buurke, A.H. Gruber, Kinematics and shock attenuation during a prolonged run on the athletic track as measured with inertial magnetic measurement units, Gait Posture 68 (2019) 155–160.
[27] Y. Zhao, J. Huang, X. He, S. Zhang, C. Ye, T. Feng, L. Xiong, Visual semantic landmark-based robust mapping and localization for autonomous indoor parking, Sensors 19 (161) (2019) 1–20.
[28] S. Bosch, B.F. Serra, M. Marin-Perianu, R. Marin-Perianu, B.J. Van der Zwaag, J. Voskamp, W. Back, R. Van Weeren, P. Havinga, Equimoves: a wireless networked inertial measurement system for objective examination of horse gait, Sensors 18 (850) (2018) 1–35.
[29] F.M. Bragana, S. Bosch, J.P. Voskamp, M. Marin-Perianu, B. Van der Zwaag, J.C. M. Vernooij, R. Van Weeren, W. Back, Validation of distal limb mounted inertial measurement unit sensors for stride detection in warmblood horses at walk and trot, Equine Vet. J. 49 (2017) 545–551.
[30] G.C. Lessi, A.F. dos Santos, L.F. Batista, G.C. de Oliveira, F.V. Serrão, Effects of fatigue on lower limb, pelvis and trunk kinematics and muscle activation: gender differences, J. Electromyogr. Kinesiol. 32 (2017) 9–14.
[31] B.C. Luz, A.F. dos Santos, M.C. de Souza, T. de Oliveira Sato, D.A. Nawoczenski, F. V. Serrão, Relationship between rearfoot, tibia and femur kinematics in runners with and without patellofemoral pain, Gait Posture 61 (2018) 416–422.
[32] A. Bevilacqua, K. MacDonald, A. Rangarej, V. Widjaya, B. Caulfield, T. Kechadi, Human activity recognition with convolutional neural networks, in: U. Brefeld, E. Curry, E. Daly, B. MacNamee, A. Marascu, F. Pinelli, M. Berlingerio, N. Hurley (Eds.), Machine Learning and Knowledge Discovery in Databases, 2019, pp. 541–552..
[33] A. Acua-Espinoza, L.F. Aragn-Vargas, Rapid changes of body weight after a headstand: a metrological analysis, PLOS ONE 10 (5) (2015) 1–9, https://doi.org/10.1371/journal.pone.0124764.
[34] A. Godfrey, R. Conway, D. Meagher, G. Laighin, Direct measurement of human movement by accelerometry, Med. Eng. Phys. 30 (10) (2008) 1364–1386, https://doi.org/10.1016/j.medengphy.2008.09.005.
[35] B. Najafi, K. Aminian, A. Paraschiv-Ionescu, F. Loew, C.J. Bula, P. Robert, Ambulatory system for human motion analysis using a kinematic sensor: monitoring of daily physical activity in the elderly, IEEE Trans. Biomed. Eng. 50 (6) (2003) 711–723, https://doi.org/10.1109/TBME.2003.812189.
[36] M. Oh, K. Hbert-Losier, S. Tuhec, V. Babi, M. Supej, Kinematics of Usain Bolt's maximal sprint velocity, Kinesiology 50 (2) (2018) 172–180, https://doi.org/10.26582/k.50.2.10.
[37] Z. Wang, J. Li, J. Wang, H. Zhao, S. Qiu, N. Yang, X. Shi, Inertial sensor-based analysis of equestrian sports between beginner and professional riders under different horse gaits, IEEE Trans. Instrum. Meas. 67 (11) (2018) 2692–2704.
[38] J.M. Bland, D.G. Altman, Statistical methods for assessing agreement between two methods of clinical measurement, Lancet 1 (8476) (1986) 307–310.
[39] M. Iwai, S. Koyama, S. Tanabe, S. Osawa, K. Takeda, I. Motoya, H. Sakurai, Y. Kanada, N. Kawamura, The validity of spatiotemporal gait analysis using dual laser range sensors: a cross-sectional study, Arch. Physiother. 9 (1) (2019) 1–8.
[40] M. Morrow, B. Lowndes, E. Fortune, K.R. Kaufman, M.S. Hallbeck, Validation of inertial measurement units for upper body kinematics, J. Appl. Biomech. 33 (3) (2017) 227–232.

[41] G. Cai, B. Chen, T. Lee, Coordinate Systems and Transformations, Springer-Verlag, 2011.
[42] N. Choe, H. Zhao, S. Qiu, Y. So, A sensor-to-segment calibration method for motion capture system based on low cost mimu, Measurement (2018) 1–21.
[43] Freescale Semiconductor, Application Note: Calibrating an eCompassin the Presence of Hard- and Soft-Iron Interference, rev. 4.0, 11/2015, 2015..
[44] H. Schwefel, G. Rudolph, Contemporary Evolution Strategies, Springer-Verlag 929 (1995) 893–907.
[45] G. Wu, S. Siegler, P. Allard, C. Kirtley, A. Leardini, D. Rosenbaum, M. Whittle, D. D'Lima, L. Cristofolini, H. Witte, S. Schmid, I. Stokes, ISB recommendation on definitions of joint coordinate system of various joints for the reporting of human joint motion'part i: ankle, hip, and spine, J. Biomech. 35 (4) (2002) 543–548.
[46] K.E. Wilk, C.A. Arrigo, Rehabilitation principles of the anterior cruciate ligament reconstructed knee: twelve steps for successful progression and return to play, Clinics Sports Med. 36 (1) (2017) 189–232, https://doi.org/10.1016/j.csm.2016.08.012.